Photoinduced Electron Transfer and Excitation Energy Transfer in Directly Linked Zinc Porphyrin/Zinc Phthalocyanine Composite

Fuyuki Ito,[†,‡,#] Yukihide Ishibashi,[†] Sazzadur Rahman Khan,[†,‡] Hiroshi Miyasaka,*[,†] Kazuya Kameyama,[§] Mitsuhiko Morisue,[§] Akiharu Satake,[§] Kazuya Ogawa,[§] and Yoshiaki Kobuke*[,§]

Division of Frontier Materials Science, Graduate School of Engineering Science, and Research Center of Materials Science at Extreme Conditions, Osaka University, Toyonaka, Osaka 560-8531, Japan, Center for Advanced Science and Innovation, Osaka University, Suita, Osaka 565-0871, Japan, and Graduate School of Material Science, Nara Institute of Science and Technology, 8916-5 Takayama, Ikoma, Nara 630-0192, Japan

Received: May 9, 2006; In Final Form: August 22, 2006

Photoinduced electron transfer (ET) and excitation energy transfer (ENT) reactions in monomer and slipped-cofacial dimer systems of a directly linked Zn porphyrin (Por)−Zn phthalocyanine (Pc) heterodyad, ZnPc−ZnPor, were investigated by means of the picosecond and femtosecond transient absorption spectroscopies. In the dimer dyad system of two heterodyads connected through the coordination bond between two imidazolyl-substituted ZnPor bearing ZnPc, ZnPc−ZnPor(**D**), the rapid ENT from the ZnPor to ZnPc in the subpicosecond time region was followed by photoinduced charge separation (CS) and charge recombination (CR) with time constants of 47 and 510 ps, respectively. On the other hand in the monomer dyad system, no clear charge-separated state was observed although the CS with a time constant of 200 ps and CR with $\leq$70 ps were estimated. These results indicated that the dimer slipped-cofacial arrangement of pair porphyrins is advantageous for the effective production of the CS state. This advantage was discussed from the viewpoint of a decrease in the reorganization energy of the dimer relative to that of the monomer system. In addition, the electrochemical measurements indicated that the strong interaction between ZnPc and ZnPor moieties also contributed to the fast CS process despite the marginal driving force for the CS process. The dimer dyad of ZnPc−ZnPor provides full advantages in efficiencies of the light harvesting and the CS state production.

Introduction

Photoinduced electron transfer (ET) processes following the excitation energy transfer (ENT) play fundamental and important roles in the natural photosynthesis.[1] A number of investigations have been performed toward the elucidation of elementary ET processes and the realization of the artificial assemblies where the conversion of the light energy takes place with high efficiency.[2−5] Most artificial systems mimicking antenna arrays and reaction centers employ chemically distinct, covalently linked chromophores with appropriate redox cofactors. Self-assembling of the chromophores, however, takes crucial roles in the natural systems to provide particular photophysical and redox properties. Construction of the molecular assemblies through weak molecular interactions may lead to the comprehensive understanding of the natural systems and to the realization of artificial systems with more efficient functions.[6]

On these molecular assemblies through weak interactions, we recently reported a complementary slipped-cofacial dimer of imidazolyl-substituted Zn porphyrin bearing an electron acceptor.[7] In the case of the dimer, the electrochemical measurements revealed that the cation radical was delocalized over the whole π-system of the dimer. Time-resolved transient absorption measurements revealed that the dimer accelerated the charge separation (CS) rate and decelerated the charge recombination (CR) process compared with those of the corresponding monomer. The major factor for these properties was the smaller reorganization energy of the slipped-cofacial dimer relative to that of the monomer system. These results indicated the significance of the special pair arrangement that contributes to the efficient charge separation in the photosynthesis.

Not only CS and CR but also light-harvesting (LH) capability is also of crucial importance in the natural photosynthetic system. Several porphyrin (Por)/phthalocyanine (Pc) composites are of interest because of their efficient light harvesting (LH) functionality in addition to the electron transfer capability. Large extinction coefficients at different wavelengths in the visible region and ideal overlap of emission and absorption spectra predict the efficient and rapid ENT processes, and various motifs of Por/Pc heterodyads were proposed and investigated.[8−10] The ET processes in porphyrin (Por)/phthalocyanine (Pc) composites were, however, rather scarcely detected and no direct proof of CS species has been presented so far, although the fluorescence lifetime measurements and redox potential of individual Por and Pc predicted the ET reaction within Por/Pc heterodyads.[10] This is probably due to a very small energy gap between the S_1 state of Pc and the charge-separated state of Por/Pc, as will be described later. For the small energy gap, formation of the charge-separated species may be slower than its reverse reaction, making the direct observation difficult. Even so, we will report

* Corresponding authors. H.M.: phone, +81-6-6850-6241; fax, +81-6-6850-6244; e-mail, miyasaka@chem.es.osaka-u.ac.jp. Y.K.: phone, +81-743-72-6110; fax, +81-743-72-6119; e-mail: kobuke@ms.naist.jp.

† Division of Frontier Materials Science, Graduate School of Engineering Science, and Research Center of Materials Science at Extreme Conditions, Osaka University.

‡ Center for Advanced Science and Innovation, Osaka University.

§ Nara Institute of Science and Technology.

Present address: Department of Applied Chemistry, Faculty of Engineering, Kyushu University. E-mail: f-ito@cstf.kyushu-u.ac.jp.

10.1021/jp062822+ CCC: $33.50 © 2006 American Chemical Society
Published on Web 11/03/2006

SCHEME 1: Molecular Structure of ZnPc−ZnPor(D) and ZnPc−ZnPor(M)

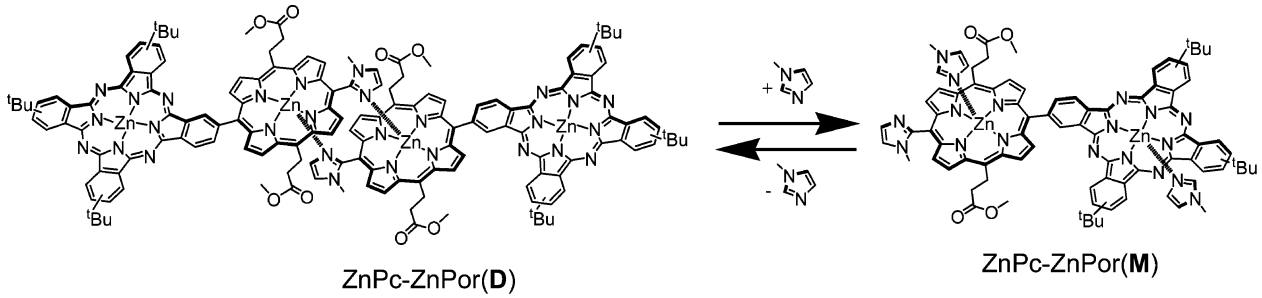

SCHEME 2: Molecular Structures of Reference Compounds Used

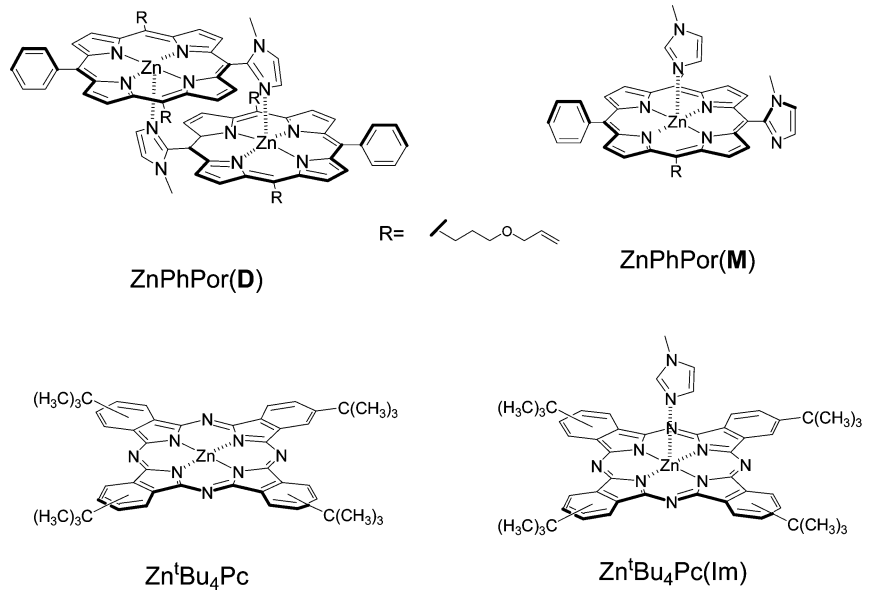

here the observation of CS species of the Pc radical cation in the Por/Pc system (Scheme 1), where Por and Pc are directly connected so as to increase the electronic coupling between these two moieties, leading to the rapid charge separation even though the energy gap is marginal.[11−14] In addition, the structure of the slipped-cofacial dimer of ZnPor was adopted to decelerate the CR rate.[7] These characteristic features of molecular structure[15] through the large dimerization constant[16] actually realized rapid CS and slow CR reactions in the ET processes. In the following, we will present the dynamic behaviors of the ZnPc−ZnPor(**D**) system as revealed by ultrafast laser spectroscopic methods. By comparing these results with those in the monomer model system, we will discuss the factors regulating the electron transfer reactions in these strongly interacting systems.

Experimental Section

Picosecond laser photolysis system with a repetitive mode-locked Nd^{3+}:YAG laser[17] combined with handmade optical parametric generation and amplification (OPGA)[18] was used for transient absorption spectral measurements. Briefly, two KDP crystals (type II, 3 cm, 61° cut) were placed close together and symmetric with respect to their optic axes to compensate the walk-off effect. The third harmonics (355 nm) was tightly focused onto the second crystal in the OPG by a cylindrical lens with a 50 cm focal length. To adjust the crystal angle of the incident laser pulse, we can cover the wavelength region between 450 and 620 nm with 0.1 mJ/pulse and ca. 16 ps fwhm. The 560 and 600 nm were used for the selective excitation of Por and Pc moieties, respectively. The excitation pulse was focused into a spot with a diameter of ca. 1.5 mm. Picosecond white continuum generated by focusing a fundamental pulse into a 10 cm quartz cell containing D_2O and H_2O mixture (3:1) was employed as a monitoring light. A sample cell with 2 mm optical length was used.

To investigate the dynamic behavior under femtosecond laser light excitation, a dual OPA laser system for kinetic transient absorption measurements was used.[19] The output of a femtosecond Ti:sapphire laser (Tsunami, Spectra-Physics) pumped by the SHG of a cw Nd^{3+}:YVO_4 laser (Millennia V, Spectra-Physics) was regeneratively amplified with 1 kHz repetition rate (Spitfire, Spectra-Physics). The amplified pulse (1 mJ/pulse energy and 85 fs fwhm) was divided into two pulses with the same energy (50%). These pulses are guided into two OPA systems (OPA-800, Spectra-Physics), respectively. OPA output pulses are converted to the SHG, THG, FHG, or sum frequency mixing with fundamental 800 nm pulse and these pulses can cover the wavelength region between 300 and 1200 nm with 1−10 mW output energy and ca. 120 fs fwhm. One of these two pulses was used as a pump light and the other one, which is reduced to <1/5000 output power, was utilized as a monitoring light. The pulse duration was estimated to be 150 fs from the cross correlation trace at the sample position. The intensities of the monitoring, reference, and pump beams were respectively monitored by photodiode detectors and sent to the microcomputer for further analysis. The sample cell with 2 mm optical length was used and the sample solution was circulated during the measurement. Fluorescence dynamics was measured by using a conventional single-photon timing apparatus with a diode picosecond laser light as an excitation source (Hamamatsu, Picosecond Light Pulser, C4725, 417 nm, 0.02 pJ/pulse, and 1

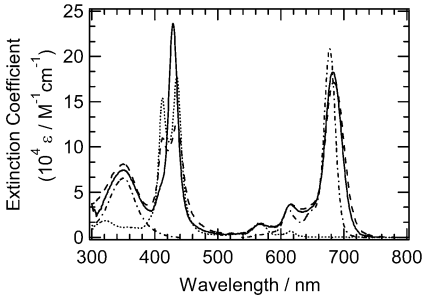

Figure 1. Absorption spectra of Zn^{t}Bu$_4$Pc (-·-), ZnPhPor(**D**) (·····), ZnPc−ZnPor(**M**) (−), and ZnPc−ZnPor(**D**) (---) system in CH_2Cl_2 solution. The extinction coefficient of the dimer species illustrates as a value per single dyad unit.

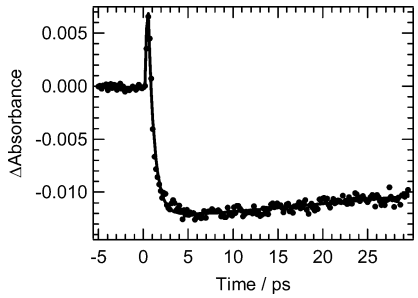

Figure 2. Time profile of the transient absorbance of ZnPc−ZnPor-(**D**) in a CH_2Cl_2 solution, excited with a 150 fs fwhm, 560 nm laser pulse, monitored at 690 nm. Solid line is the calculated curve convoluted with the pulse duration.

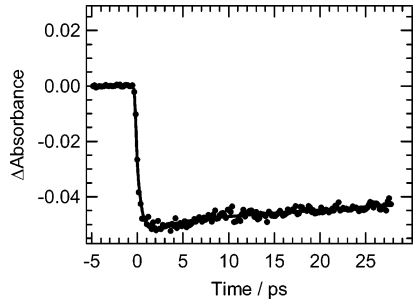

Figure 3. Time profile of the transient absorbance of ZnPc−ZnPor-(**M**) in a CH_2Cl_2 solution, excited with a 150 fs fwhm, 560 nm laser pulse, monitored at 690 nm. Th solid line is the calculated curve based on the exponential function convoluted with the pulse duration.

MHz repetition rate). All the measurements were performed under O_2-free conditions at 22 ± 2 °C.

Synthetic detail of ZnPc−ZnPor was reported in the previous paper.[15] Dichloromethane (Wako, infinity pure grade) was used as a solvent without further purification. The HOMO−LUMO levels were determined by cyclic voltammetry (BAS CV-50W potentiostat) of the corresponding ZnPhPor and Zn^{t}Bu$_4$Pc units illustrated in Scheme 2 in CH_2Cl_2 using 0.1 M nBu$_4$NPF$_6$ as supporting electrolyte.

Results and Discussion

Absorption Spectra in the Ground State. Steady state absorption spectra of Zn^{t}Bu$_4$Pc and ZnPhPor(**D**) as reference samples, whose molecular structures are shown in Scheme 2, ZnPc−ZnPor(**M**), and its dimer ZnPc−ZnPor(**D**) are exhibited in Figure 1. The spectrum of ZnPhPor(**D**) shows a very strong Soret band around 410 nm and Q-bands in the range 510−650 nm. Zn^{t}Bu$_4$Pc has strong bands around 350 nm (Soret band) and in the range 600−700 nm (Q-bands). The constant for self-association of ZnPhPor is $\sim 10^{11}$ M^{-1};[16] thus the spectrum of ZnPc−ZnPor(**M**) was measured with 0.1 M 1-methylimidazole in CH_2Cl_2 to avoid the self-association. Although the spectrum of ZnPc−ZnPor(**M**) is close to the superposition of these two absorption spectra of ZnPhPor(**M**) and Zn^{t}Bu$_4$Pc, one can find that the Q-band of Pc and the Soret band of Por of ZnPc−ZnPor(**M**) system are broadened significantly. These broad bands suggest rather strong interaction between Por and Pc moieties in this dyad. In the absence of 1-methylimidazole, ZnPc−ZnPor(**M**) forms dimer dyad ZnPc−ZnPor(**D**), which is composed of two ZnPc−ZnPor(**M**)'s coordinated between zinc ion and imidazolyl substituted at the meso position.[15] In addition to the broadening, the spectrum of the dimer dyad, ZnPc−ZnPor(**D**), shows the splitting of Soret band at 413 and 437 nm. This splitting indicates the self-assembled dimerization of ZnPc−ZnPor.[6,7,15] This splitting is explained by the exciton splitting theory proposed by Kasha.[20]

The fluorescence properties of ZnPc−ZnPor(**D**) and -(**M**) and Zn^{t}Bu$_4$Pc are depicted in the previous report.[15] Briefly, the fluorescence only from Pc moieties was observed even in the excitation of Por moieties and no fluorescence was observed from the Por part in ZnPc−ZnPor(**M**) and -(**D**), suggesting the rapid ENT from the excited Por to the Pc moiety in these systems. In addition, the fluorescence quantum yield (Φ_F) of the PC moiety decreases with increasing solvent dielectric constant. The Φ_F values are 0.16, 0.090, 0.025 for ZnPc−ZnPor-(**D**) and are 0.25, 0.18, 0.12 for ZnPc−ZnPor(**M**) in toluene ($\epsilon = 2.38$), chloroform ($\epsilon = 4.81$), and dichloromethane ($\epsilon = 9.08$), respectively. These values are much smaller than those for the reference system of Zn^{t}Bu$_4$Pc, of which Φ_F are 0.30, 0.39, and 0.40 in toluene, chloroform, and dichloromethane, respectively. From the solvent polarity dependence of Φ_F of the dyad systems, fluorescence quenching due to the electron transfer reaction is strongly suggested for both the monomer and dimer dyad systems.

Excitation Energy Transfer Process. Prior to the discussion on the electron transfer processes, we present the excitation energy transfer (ENT) dynamics in the dyad system. Figure 2 shows the time profile of the transient absorbance at 690 nm of ZnPc−ZnPor(**D**) in a CH_2Cl_2 solution, following the selective excitation of ZnPor moiety at 560 nm with a 150 fs laser pulse. Positive absorption around the time origin is ascribed to the $S_n \leftarrow S_1$ absorption of ZnPor,[14] which is replaced with a negative absorption due to bleaching of ZnPc. The time profile of the transient absorbance could be reproduced with a decrease of the positive absorbance to the negative one with $\tau = 0.67 \pm 0.10$ ps, and the recovery process of the negative absorption with a much longer time constant. As will be discussed in the section of the electron transfer dynamics, this recovery process was reproduced by the biphasic decay process with $\tau = 25 \pm 5$ ps and 690 ± 100 ps. The appearance of the negative absorption due to the bleaching of ZnPc could be ascribed to the ENT from the ZnPor moiety to the ZnPc moiety.

In the time profile of transient absorbance at 690 nm of ZnPc−ZnPor(**M**) in a CH_2Cl_2 solution excited with 560 nm in Figure 3, the negative absorption appears just after the excitation due to the bleaching signal of ZnPc and no positive absorption immediately after the excitation was observed. This might be due to the rather small extinction coefficient of the S_1 state of the ZnPor monomer moiety and faster time constant of the ENT process compared to the time profile of the ZnPc−ZnPor(**D**). Actually, the time constant of the appearance of the negative signal was obtained to be ≤0.5 ps. The recovery process of the negative absorption was reproduced by the biphasic decay process with $\tau = 30 \pm 10$ ps and 400 ± 100 ps and will be

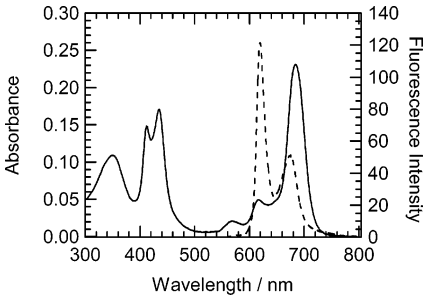

Figure 4. Absorption spectra of ZnPc−ZnPor(**D**) (solid line) and fluorescence spectra of ZnPhPor (hashed line) excited at 413 nm in a CH_2Cl_2 solution.

discussed later. Anyhow, the above results indicate that the ENT processes from ZnPor to ZnPc moieties in these dyad systems take place with time constants <1 ps, as predicted in the steady state fluorometry.[15]

To evaluate these rapid ENT processes, we estimate the rate constant in the framework of the Förster's model.[21−24] The rate constant could be represented by

$$k_{ENT} = \frac{9000 \cdot \ln 10 \cdot \kappa^2 \Phi_D}{128\pi^5 n^4 N \tau_D R^6} J = \frac{8.8 \times 10^{-25} \cdot \kappa \cdot \Phi_D}{n^4 \tau_D R^6} J \quad (1)$$

where κ^2 is the orientation factor, Φ_D is the donor fluorescence quantum yield in the absence of acceptor, J is the overlap integral, n is the index of refraction of the solvent, N is Avogadro's number, τ_D is the donor fluorescence lifetime in the absence of acceptor, and R is the interchromophoric distance (in cm). The overlap integral J ($cm^6\ mol^{-1}$) is given by

$$J = \int f_D(\nu)\, \epsilon_A(\nu)\, \nu^{-4}\, d\nu \quad (2)$$

where $f_D(\nu)$ is the normalized fluorescence spectra of the donor, $\epsilon_A(\nu)$ is the absorption spectrum of the energy acceptor with molar extinction coefficient ($M^{-1}\ cm^{-1}$). The value of $J = 1.11 \times 10^{-12}\ cm^6\ mol^{-1}$ was obtained from eq 2 on the basis of the absorption and emission spectra of reference Por and ZnPc−ZnPor(**D**) shown in Figure 4, suggesting the strong dipole−dipole interaction between ZnPc and ZnPor through the overlap of ZnPor emission and ZnPc absorption. The critical distance R_0 between the two molecules such that the energy transfer probability equals the fluorescence probability is defined by the following equation.

$$R_0 = \sqrt[6]{\frac{8.8 \times 10^{-25} \cdot \kappa^2 \cdot \Phi_D \cdot J}{n^4}} \quad (3)$$

The critical distance thus estimated in the present ZnPor and ZnPc pair was 48 Å, which is comparable to other Pc−Por dyad systems.[10b]

The energy transfer rate constant was calculated to be $k_{ENT} = 2.00 \times 10^{12}\ s^{-1}$, $(500\ fs)^{-1}$, with $\Phi_D = 0.14$,[15] $n = 1.42$ for dichloromethane,[25] $\tau_D = 2.5$ ns,[24] and $R = 12$ Å (center-to-center distance estimated by the PM3 calculation), even under the condition that the κ^2 value is assumed to be $^2/_3$ (random orientation). In addition, κ^2 could be to be estimated 3.06 (where $\kappa^2 = (\cos\theta_T - 3\cos\theta_i \cos\theta_j)^2$, $\theta = 120°$) and $k_{ENT} = 9.18 \times 10^{12}\ s^{-1}$, $(110\ fs)^{-1}$, by taking into account the transition moments of porphyrin and phthalocyanine, which are considered to direct along trans meso positions and trans phenyl groups, respectively. This value is roughly in agreement with the experimental result of the time profile of transient absorbance

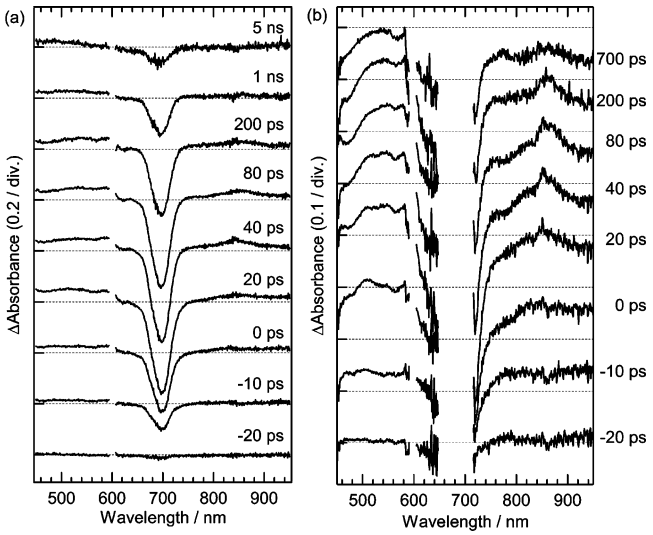

Figure 5. Time-resolved transient absorption spectra of ZnPc−ZnPor(**D**) in a CH_2Cl_2 solution, excited with a 16 ps fwhm laser pulse at 600 nm. The solution concentrations are (a) $4.4 \times 10^{-5}\ mol \cdot dm^{-3}$ and (b) $1.0 \times 10^{-4}\ mol \cdot dm^{-3}$.

of the ZnPc−ZnPor system excited with 560 nm. In addition, the directly connected systems may induce the electronic exchange interaction by direct or indirect overlap of wave functions.[25] In any event, the above estimation indicates that the very rapid excitation energy transfer is predicted even in the framework of Förster mechanism. The energy transfer rate constant in the ZnPc−ZnPor(**M**) system is faster than that in the ZnPc−ZnPor(**D**) system from transient kinetic measurements, in accord with the indication that the interaction between Por and Pc is stronger in ZnPc−ZnPor(**M**) than in ZnPc−ZnPor(**D**), judged by the broader absorption line width of the former Pc moiety compared with the latter (600−740 nm in Figure 1).

Time-Resolved Detection of the Electron Transfer Dynamics. To directly clarify the electron transfer dynamics, transient absorption spectroscopy was applied by using picosecond laser pulses at 560 and 600 nm. Figure 5 shows transient absorption spectra of ZnPc−ZnPor(**D**) in CH_2Cl_2 solution excited with a 16 ps laser pulse at 600 nm. The wavelength at 600 nm corresponds to the selective excitation of the ZnPc moiety. To detect reatively weak positive absorption signals, a concentrated solution of ZnPc−ZnPor(**D**) was used in Figure 5b. A negative absorption band with a maximum at 690 nm appearing within the response function at 600 nm is safely ascribed to the bleaching signal of the ZnPc in the ground state. In the few tens of picoseconds time region, a positive absorption around 850 nm and dip signals around 570 and 620 nm gradually appear. The absorption around 850 nm is ascribed to the cation radical of ZnPc ($ZnPc^{\bullet+}$) on the basis of the absorption maximum and spectral band shape of the reference spectrum.[26] On the other hand, the dip signals around 570 and 620 nm are ascribable to the bleaching signal of ZnPor in the ground state. The evolution of these absorption signals indicates that the charge separation (CS) between the excited ZnPc and ZnPor takes place in the few tens of picoseconds time region. It should be mentioned that the absorption[27] of $ZnPor^{\bullet-}$ around 450 nm is not clearly observed. This may be due to the strong absorption of the Soret band as shown in Figure 1. Namely, the superimposition of the negative signal due to the bleaching of the strong Soret band on the positive signal of $ZnPor^{\bullet-}$ prohibits the detection of the absorption of $ZnPor^{\bullet-}$. With an increase in the delay time after the excitation, the absorption due to $ZnPc^{\bullet+}$ and dip signals around 570 and 620 nm gradualy decay and

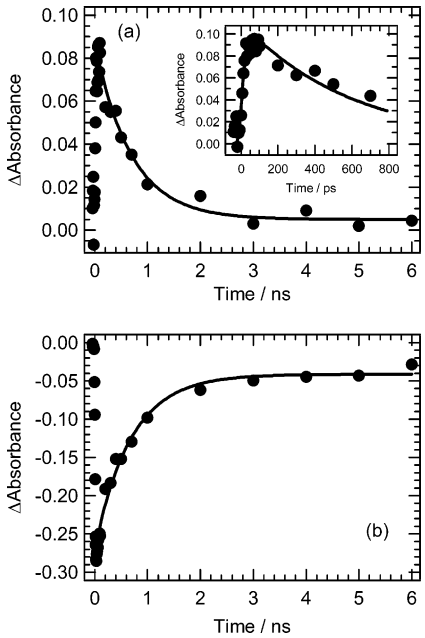

Figure 6. Time profile of the transient absorbance of ZnPc−ZnPor-(**D**) in a CH_2Cl_2 solution, excited with a 16 ps fwhm, 600 nm laser pulse, and monitored at 850 nm (a) and 690 nm (b). The inset shows the expanded time profile until 800 ps after the excitation. The solid line of the inset is the convolution curve calculated on the basis of the pulse widths of the pump and the probe pulse (16 ps) and 25 ps rise and 690 ps decay time constants, and the solid line of (b) is calculated by biphasic decay with time constants of 25 and 690 ps.

weak positive absorption remains with a negative signal at ca. 700 nm at 6 ns following the excitation. This spectrum is assigned to $T_n \leftarrow T_1$ absorption of the ZnPc[28,29] on the basis of the spectral band shape. This result implies that the recombination of the CS state resulted partly in the intersystem crossing, but the contribution seems less significant. If anything, the fact indicates that the energy level of the CS state is higher than that of the triplet state of ZnPc−ZnPor(**D**).

Figure 6 shows the time profiles of ZnPc−ZnPor(**D**) in CH_2Cl_2 solution monitored at 850 and 690 nm after the picosecond 600 nm laser excitation. The time profile at 850 nm (Figure 6a), which corresponds to $ZnPc^{\bullet+}$ shows the appearance of the positive absorbance in the several tens of picoseconds region, followed by the decay in the subnanosecond−nanosecond time region. The solid line is a curve calculated on the basis of the durations of the exciting and monitoring pulses and time constants of rise and decay components of 25 ± 5 and 690 ± 100 ps, respectively.

The time profile of the recovery of the ground state bleaching at 710 nm is shown in Figure 6b. The negative absorption appearing with the response function of the apparatus is followed by the biphasic recovery with time constants of τ = 25 ± 5 and 690 ± 100 ps. The fast decay of 25 ± 5 ps may be interpreted as due to the difference of the extinction coefficients between ZnPc* and $ZnPc^{\bullet+}$. Namely, the extinction coefficient of $ZnPc^{\bullet+}$ may be larger than that of ZnPc* around 690 nm. In addition, the decrease of the stimulated emission of the S_1 state of ZnPc by the monitoring light can lead to the decay of the negative absorption signal with the CS state production. On the other hand, the longer decay time of 690 ± 100 ps was almost the same with the decay time constant observed at 850 nm, indicating that the recovery of the bleaching is due to the CR process. The offset component with 10% remaining until 6 ns is ascribed to the triplet state of ZnPc. The residual signal of the triplet implies that part of the CR process leads to the intersystem crossing, as stated in the explanation of Figure 5. The same temporal evolution in the picosecond to nanosecond time region confirmed also in the case that the picosecond laser pulse at 560 nm was employed for the selective excitation of the ZnPor moiety, indicating that the electron transfer reactions actually took place after the rapid ENT.

To explore the dynamic behaviors more precisely, the temporal evolution of the fluorescence was also investigated. Figure 7 shows the time profile of the fluorescence of ZnPc−ZnPor**(D)** in CH_2Cl_2 solution, excited with a 417 nm picosecond laser light and monitored the emission of ZnPc moiety in the wavelength region >700 nm. The time profile was analyzed by triphasic decay process. Time constants and amplitude factors for the curve in Figure 7 were 40 ps (69%), 600 ps (28%), and 4.5 ns (3%), respectively. The longest time constant was set to be the same with the time constant of the free ZnPc moiety without ZnPor, meaning that the small amount of the ZnPC was involved in the present measurement.[30] Because the instrumental response function (IRF) of the picosecond light pulse in the present measurement was 80 ps (fwhm of the laser pulse), the time constant and the amplitude factors may be less reliable compared to those in the transient absorption spectroscopy. The time profile of the fluorescence, however, indicated that the major component of the fluorescence decay was 40 ps, and this fast decay was followed by the component of 600 ps. From the iterative simulation for the time profile, the fast and the second time constant were estimated to be 40 ± 10 and 630 ± 30 ps, respectively, and these time constants were consistent with those obtained by the transient absorption spectroscopy, 25 ± 10 and 690 ± 50 ps. As will be mentioned later, the energy level of the CS state is estimated to be very close to the S_1 level of of ZnPc. Hence, the above results indicate that the excited state of ZnPc moiety and the charge-separated state are in the rapid equilibrium.

For the system with equilibrium between the locally excited (LE) state and charge-separated (CS) state (Scheme 3), the dynamic behaviors of the LE state and CS state can be represented by the following equations.[14,31]

$$[\mathrm{LE}(t)] = \frac{[\mathrm{LE}(0)]}{\beta - \alpha}[(\beta - \mu)\cdot\exp(-\alpha t) + (\mu - \alpha)\cdot\exp(-\beta t)] \quad (4)$$

$$[\mathrm{CS}(t)] = \frac{k_{\mathrm{CS}}}{\beta - \alpha}[\exp(-\alpha t) - \exp(-\beta t)] \quad (5)$$

$$\alpha = \frac{1}{2}\{(\nu + \mu)^2 - \sqrt{(\nu - \mu)^2 + 4k_{\mathrm{CS}}k_{-\mathrm{CS}}}\} \quad (6)$$

$$\beta = \frac{1}{2}\{(\nu + \mu)^2 + \sqrt{(\nu - \mu)^2 + 4k_{\mathrm{CS}}k_{-\mathrm{CS}}}\} \quad (7)$$

$$\mu = k_{\mathrm{f}} + k_{\mathrm{CS}} \quad (8)$$

$$\nu = k_{\mathrm{CR}} + k_{-\mathrm{CS}} \quad (9)$$

Here, k_{CS} is the rate of CS, $k_{-\mathrm{CS}}$ the rate of reverse electron transfer to generate LE state, and k_{f} the fluorescence lifetime of the ZnPc moiety $(4.5\ \mathrm{ns})^{-1}$. The CS and CR time constants corresponding to $(k_{\mathrm{CS}})^{-1}$ and $(k_{\mathrm{CR}})^{-1}$ were respectively obtained to be 47 ± 10 and 510 ± 50 ps by the analysis of the time profile of the fluorescence on the basis of the above scheme and equations. In addition, the time constant of the back CS reaction in the excited state, $(k_{-\mathrm{CS}})^{-1}$, was 120 ± 30 ps.

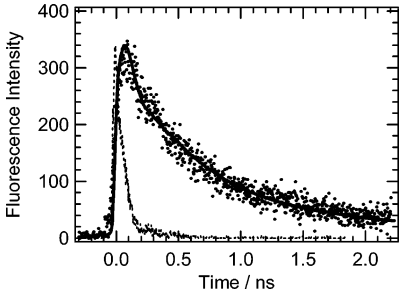

Figure 7. Fluorescence decay of ZnPc−ZnPor(**D**) in CH_2Cl_2 solution excited with 417 nm laser light and monitored at >700 nm. The dotted line is the scattering of the 417 nm laser light, and the solid line is the result based on the triphasic decay (see text).

SCHEME 3: Diagram of the CS State near the LE State

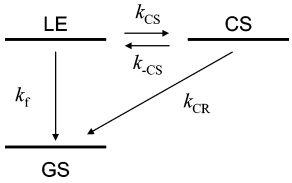

Figure 8 shows transient absorption spectra of the monomer dyad, ZnPc−ZnPor(**M**), in CH_2Cl_2 solution, excited with a picosecond 600 nm laser pulse. The monomer dyad was prepared by the addition of excess 1-methylimidazole (Im, 0.1 M) into the CH_2Cl_2 solution[15] of ZnPc−ZnPor(**D**) to break the coordination between ZnPor's. As was observed in the dimer system of ZnPc−ZnPor(**D**), negative absorption around 700 nm due to the bleaching of the ZnPc in the ground state appears immediately after the excitation with a response of the laser pulse, together with the appearance of the positive absorption bands in the wavelength region <620 nm and a negative dip signal at 780 nm. The positive signals shorter than 620 nm can be assigned to the $S_n \leftarrow S_1$ absorption[9e] of ZnPc and the negative absorption signal at 780 nm is ascribable to the stimulated emission of ZnPc. The transient absorption spectra in the early stage after the excitation indicate that the main component of the transient species is the excited singlet state of ZnPc and the positive absorption around 850 nm due to $ZnPc^{\bullet+}$ was not observed in the ZnPc−ZnPor(**M**) system. as indicated in Figure 8b, where the transient spectra of the dimer dyad and the monomer dyad at 80 ps after the excitation were plotted. With an increase in the delay time after the excitation, these absorption signals decay and a weak transient absorption remains at 6 ns after the excitation. The positive absorption around at 6 ns is ascribed to the $T_n \leftarrow T_1$ transition of the ZnPc.[28]

The time profile of the ground state recovery of ZnPc−ZnPor-(**M**) monitored at 710 nm is shown in Figure 9. The solid line is the curve calculated on the basis of the biexponential function with $\tau = 30 \pm 10$ and 400 ± 100 ps. As stated in the previous sections, the solvent polarity dependence of the fluorescence intensity in ZnPc−ZnPor(**M**) strongly suggested the electron transfer quenching process. The transient absorption spectra, however, did not indicate the CS state although the decay of the S_1 state was much faster than the decay of the monomer system without ZnPor. This result strongly implies that the CR process is much faster than the production of the CS state. To elucidate the dynamic behaviors more precisely, the time profile of the fluorescence was also measured by the single-photon timing.

Figure 10 shows the fluorescence time profile of the ZnPc−ZnPor**(M)** in CH_2Cl_2 solution, excited with a 417 nm picosecond laser light and monitoring the emission of the ZnPc moiety in the wavelength region >700 nm. The time profile was analyzed by the triphasic decay process in the same manner as for the dimer dyad. The time constants and amplitude factors for the curve in Figure 10 were 30 ps (8%), 400 ps (77%), and 4.5 ns (15%), respectively. From the iterative simulation for the time profile, the fast and the second time constant were estimated to be 30 ± 10 and 400 ± 30 ps. These time constants were almost identical to those obtained by transient absorption spectroscopy (Figure 9). The energy level of the LE state of the ZnPc moiety and the CS state at ZnPc−ZnPor(**M**) are also nearly the same, implying the rapid equilibrium between the LE state and the CS state. However, the time profile of the fluorescence for the

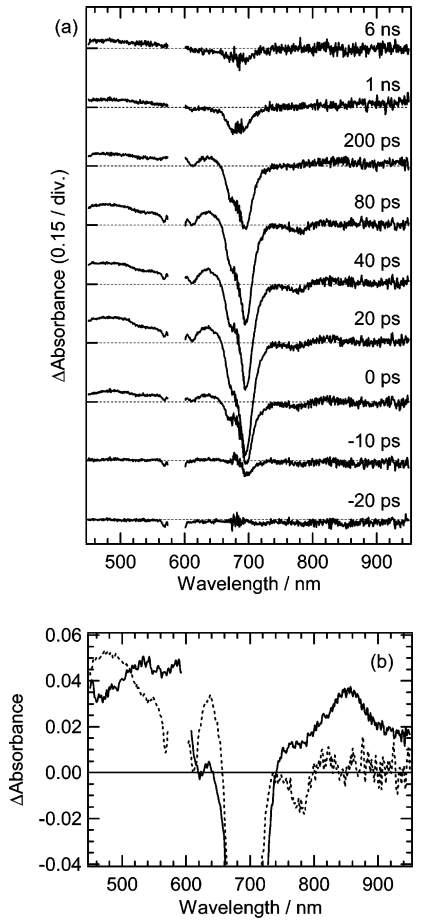

Figure 8. (a) Time-resolved transient absorption spectra of ZnPc−ZnPor(**M**) in a CH_2Cl_2 solution, excited with a 15 ps fwhm laser pulse at 600 nm. (b) Time-resolved transient absorption spectra of ZnPor−ZnPC(**D**) (solid line) and ZnPor−ZnPC(**M**) (dotted line) in a CH_2Cl_2 solution, observed at 80 ps after the excitation with a 16 ps fwhm, 600 nm laser pulse.

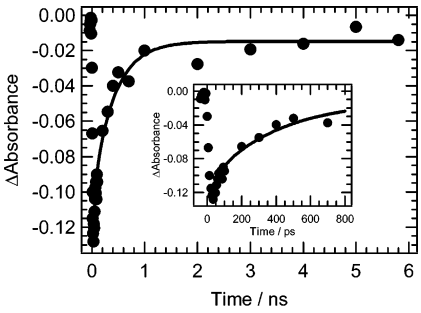

Figure 9. Time profile of the transient absorbance of ZnPc−ZnPor-(**M**) monitored at 710 nm. The solid line indicates the calculated curve by a double exponential function with time constants of 30 and 400 ps. Inset: an expanded time profile until 800 ps after the excitation.

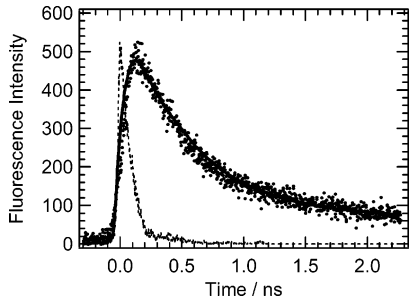

Figure 10. Fluorescence decay of ZnPc−ZnPor(**M**) in CH_2Cl_2 solution excited with 417 nm laser light and monitored at >700 nm. The dotted line is the scattering of the 417 nm laser light, and the solid line is the result based on the triphasic decay (see text).

TABLE 1: Oxidation Potential (E_{ox}), Reduction Potential ($E_{red.}$), 0−0 Transition Energy Gaps (E_S), and Energy Gaps of Charge Separation ($-\Delta G_{CS}$) and Recombination ($-\Delta G_{CR}$) of ZnPhPor and Zn^{t}Bu$_4$Pc in CH_2Cl_2

		$E_{ox.}$/V	$E_{red.}$/V	E_S/eV	$-\Delta G_{CS}$/eV	$-\Delta G_{CR}$/eV
ZnPhPor(**D**)	A^-	+0.63	−1.52	2.0	very small	1.84
Zn^{t}Bu$_4$Pc	D^+	+0.40	ND	1.8	(−0.04)	
ZnPhPor(**M**)	A^-	+0.56	−1.52	2.0	very small	1.95
Zn^{t}Bu$_4$Pc(Im)	D^+	+0.56	ND	1.8	(−0.14)	

ZnPc−ZnPor(**M**) system indicated that the fast 30 ps component of fluorescence decay has a small contribution, and the main component is the subsequent time constant with 400 ps. The ratio of ca. 1/10 for pre-amplitudes of the fast (30 ps) and the slow (400 ps) components of ZnPc−ZnPor(**M**) system matches the indication that the rate constant of CR is faster than that of CS even in the case where the electron transfer process is responsible for the quenching of the monomer dyad. The CS and CR time constants corresponding to $(k_{CS})^{-1}$ and $(k_{CR})^{-1}$ were estimated to be 200 ± 20 and 66 ± 10 ps, respectively, by the analysis of the time profile of the fluorescence on the basis of the above scheme assuming the equilibrium between ZnPc* and CS states.

Energy Gaps for the Electron Transfer Reactions. Energy gaps for the electron transfer, $-\Delta G_{CS}$ and $-\Delta G_{CR}$ of ZnPhPor dimer, ZnPhPor and Zn^{t}Bu$_4$Pc monomers in CH_2Cl_2 were estimated from the 0−0 transition energy gap (E_S) between the lowest excited state and the ground state, the oxidation potential ($E_{ox.}$), and the reduction potential ($E_{red.}$) as listed in Table 1. This standard potential did not shift even if 1-methylimidazole was added.

The driving force $-\Delta G_{CR}$ for intramolecular CR process from the ZnPor radical anion to the ZnPc radical cation was calculated from the following equations.[32]

$$-\Delta G_{CR} = E_{ox.} - E_{red.} + \Delta G_S \tag{10}$$

$$\Delta G_S = \frac{-e^2}{4\pi\epsilon_0\epsilon R_{DA}} \tag{11}$$

Here, R_{DA} is the distance of ion pair, ϵ and ϵ_0 are dielectric constants of the solvent and of the vacuum, respectively, and e stands for elementary charge. In the present system, ΔG_S was obtained as −0.134 eV with $\epsilon = 8.39$ (dichloromethane at 298 K) and R_{DA} = 1.2 Å. The driving force $-\Delta G_{CS}$ for the intramolecular CS process from ZnPc to ZnPor was roughly estimated by eq 12, and these results were summarized in Table 1.

$$-\Delta G_{CS} = E_S - \Delta G_{CR} \tag{12}$$

Oxidation and reduction potentials ($E_{ox.}$ and $E_{red.}$) of self-assembled the ZnPhPor dimer unit were +0.63 and −1.52 V (vs Ag/AgCl), respectively. $E_{ox.}$ of Zn^{t}Bu$_4$Pc was obtained as +0.4 V. The energy gap of charge recombination, ΔG_{CR}, from the CS state to the ground state of ZnPc−ZnPor(**D**) is −1.79 eV, and the 0−0 transition energy of zinc ^{t}Bu$_4$Pc, E_S, is 1.8 eV. The energy level diagram estimated by the electrochemical and spectroscopic data of the ZnPc−ZnPor system is summarized in Scheme 4 with time constants and quantum yields. ZnPc−ZnPor(**D**) has large extinction coefficients in the almost entire visible wavelength region. Thus, the visible light energy is captured effectively by the porphyrin and phthalocyanine moieties. The energy captured by the porphyrin part is transferred into the phthalocyanine part almost quantitatively with a time constant of 0.7 ps. Therefore, all of the light energy captured by ZnPc−ZnPor(**D**) is converged in the excited phthalocyanine. Subsequently, the excited ZnPc*−ZnPor(**D**) is converted into the CS state, $ZnPc^{\bullet+}$−$ZnPor^{\bullet-}$(**D**), via electron transfer in a 93% yield, which is estimated by $1 - \Phi_F/\Phi_F^\circ$, where Φ_F and Φ_F° are the fluorescence quantum yields of ZnPc−ZnPor(**D**) and Zn^{t}Bu$_4$Pc (0.40). It is noted that $-\Delta G_{CR}$ and E_S are nearly the same, leading the marginal driving force for charge separation, because the energy gap of the CS and CR reactions is shared in the S_1 state energy of 1.8 eV. Even with such a small energy gap, a rapid electron transfer is achieved very efficiently. Because of the smallest energy gap of $-\Delta G_{CS}$, the maximum energy level is maintained at the CS state, from which charge recombination occurs with a time constant of 510 ± 50 ps. The high energy level of the CS state offers distinct advantages in terms of the eficient utilization of photoexcitation energy and depressing of the CR rate by the energy gap law. Actually, because the CR process is more than 10 times slower than the CS process, enough opportunity arises to use the high energy ion pair as a photovoltaic system.

Analysis of k_{CS} and k_{CR} in the Framework of the Nonadiabatic ET Reaction. As estimated in the previous section, the energy gap for the CR, $-\Delta G_{CR}$ (1.79 eV), and 0−0 transition energy, E_S (1.8 eV), are nearly the same, leading to the marginal driving force for charge separation. On the factors enabling the CS rate constant of $\sim 2 \times 10^{10}$ s^{-1} for such a small energy gap for the CS process, we first discuss these electron transfer rate constants in the ZnPc−ZnPor system within the framework of the nonadiabatic electron transfer theory. The well-known expression in the above framework is given in eqs 13−15.[33,34] Here, V is the electronic coupling matrix element,

$$k_{ET} = \sqrt{\frac{\pi}{\hbar^2\lambda_s k_B T}}|V|^2\sum_0^\infty\left(\frac{e^{-S}S^n}{n!}\right) \times \exp\left[-\frac{(\lambda_s + \Delta G + n\hbar\langle\omega\rangle)^2}{4\lambda_s k_B T}\right] \tag{13}$$

$$S = \frac{\lambda_v}{\hbar\langle\omega\rangle} \tag{14}$$

$$\lambda_s = e^2\left(\frac{1}{2r_A} + \frac{1}{2r_D} - \frac{1}{R}\right)\left(\frac{1}{n^2} - \frac{1}{\epsilon}\right) \tag{15}$$

$S = \lambda_v/\hbar\langle\omega\rangle$ is the electron-vibration coupling constant, λ_v is the reorganization energy associated with the averaged angular frequency $\langle\omega\rangle$, and λ_s is the solvent reorganization energy. Figure 11 shows semilogarithmic plots of k_{CS} and k_{CR} against ΔG_{CS} and ΔG_{CR} for the ZnPc−ZnPor systems and the calculated

SCHEME 4: Energy Level Diagram of ZnPc−ZnPor(D)

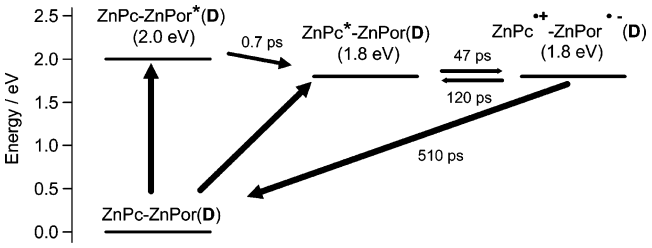

curves by eq 13 in CH_2Cl_2 ($n = 1.42$, $\epsilon = 8.93$ at room temperature[26]). In this plot, the CS and CR time constants of the monomer dyad were respectively set to 200 and 30 ps. We used a value of 1500 cm^{-1} for $\langle\omega\rangle$ on the basis of the porphyrin macrocycle C═C double-bond frequency, and the λ_v value of 0.3 eV, obtained for the CS reaction of the porphyrin-imide dyad systems.[14] The energy gap dependence of the ET rate constants in ZnPc−ZnPor(**M**) and -(**D**) were analyzed by adjusting only the λ_s value with other parameters fixed; the results for $\lambda_s = 0.42$ eV for ZnPc−ZnPor(**M**) and $\lambda_s = 0.32$ eV for ZnPc−ZnPor(**D**) are shown by the dotted and solid lines in Figure 11. The λ_s value for ZnPc−ZnPor(**M**) is estimated by eq 15 with $r_A = 5.0$ Å, $r_D = 7.5$ Å, and $r_{DA} = 11.0$ Å. The λ_s value for ZnPc−ZnPor(**D**) is lower than that for ZnPc−ZnPor(**M**) by approximately 0.1 eV, which was estimated from the analogy in the previous paper on the dimer dyad of the porphyrin−imide system,[7] where it was revealed that the dimer porphyrin delocalizes the cationic state leading to the decrease of the reorganization energy and facilitating the rapid CS and slow CR rates. The present result in Figure 11 strongly suggests that not only the cation but also the anion radical are delocalized over two porphyrin π-orbitals to favor the CS state.

The parameter $V = 16$ meV for both ZnPc−ZnPor(**M**) and -(**D**) indicates that the electronic interaction in the present systems is considerably large compared to other intramolecular porphyrin−electron donor/acceptor systems.[35] The large V value might account for the short D−A distance through direct connection. Actually, the V value of the directly connected porphyrin−imide system[14] was reported to be 14 meV and comparable to that for the present system. The above discussion indicates that large V values and smaller reorganization energy in the dimer system allow the rapid CS process in the dimer dyad.

Although several Por/Pc heterodyad systems have been reported,[8−10] no direct observation of the ET reaction between Por and Pc has been presented. The reason for the lack of the direct detection of the CS state is probably due to the rather low energy of the S_1 state of Pc (∼1.8 eV), leading to the restrictions for the optimization of the redox factor for the energy gaps in the electron transfer processes. Namely, the large energy gap for the charge separation (CS) decreases the energy gap for the charge recombination (CR). The largest rate for the CS process is expected to be observed at the condition that the energy gap for the CS is around the reorganization energy. Because the typical reorganization energy in polar or medium polar environments is ca. 0.5−1.0 eV, the energy gap for the fast CS rate also corresponds to the fast CR rate for the electron transfer processes in Pc systems. On the other hand, the large energy gap for the CR process reduces both the CS and CR rate constants, leading to the difficulty in the observation of the CS state in the dynamic measurement. The present system overcomes the incompatibility problem by accelerating the CS process of very small energy gap.

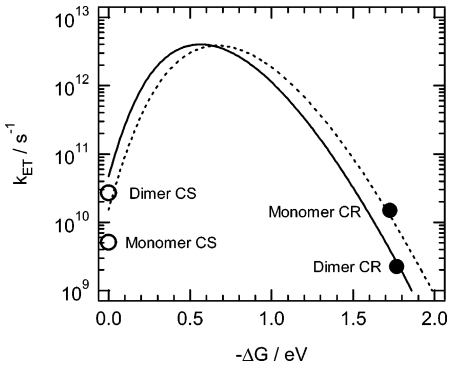

Figure 11. Energy gap dependence of k_{CS} and k_{CR} for ZnPor−ZnPc dyads. The curves were calculated by eq 13, with $T = 295$ K, $\lambda_v = 0.3$ eV, $V = 16$ meV, $\hbar\langle\omega\rangle = 0.15$ eV, and $\lambda_s = 0.42$ (dotted line) and 0.32 eV (solid line) for ZnPor−ZnPc(**M**) and ZnPor−ZnPc(**D**), respectively.

ET Dynamics with Stronger Interchromophore Electronic Interaction. As discussed in the previous section, the rather large electronic interaction between ZnPor and ZnPc and the decrease in the reorganization energy by the dimerization lead to the acceleration of CS and deceleration of CR. In addition, the broadening of the absorption spectra in the ground state and the rapid energy transfer from ZnPor to ZnPc suggest the presence of other favorable factors enabling the efficient and fast CS ($k_{CS} > \sim 10^{10}$) even in the marginal driving force, $\Delta G_{CS} \sim 0$. Namely, the broadened absorption in the ground state of ZnPor−ZnPC**(D)**, as was shown in Figure 1, strongly suggests the CT interaction. In addition, the rapid excitation energy transfer also suggested the strong interaction between the excited states of ZnPc and ZnPor by the direct connection of these moieties. The presence of strong interaction through the CT as well as excited states may lead to the acceleration of the production of the CS state as exciplexes such as pyrene-*N*,*N*-dimethylaniline and anthracene-*N*,*N*-dimethylaniline in nonpolar solvents. In these systems, the charge-separated species are produced with large bimolecular rate constants as comparable as the diffusion-limited rate even though the energy level of the CS state estimated by electrochemical data is much higher than the S_1 state level.[36,37] For this rapid production of the charge-separated state, the strong interaction through the charge resonance and exciton resonance has been considered to take an important role.[38] Although the present system does not have a geometry as in the exciplex systems in nonpolar solvents (sandwich-type between two π-planes), the direct connection of electron donor and acceptor and the overlap of the emission of ZnPor moiety and the strong absorption of ZnPc in the present case may allow the strong interaction through the electron exchange, leading to the acceleration of the CS reaction.

Concluding Remarks

The following observations were obtained: (1) ZnPc−ZnPor-(**D**) is an efficient light-harvesting complex, in which all four chromophores absorb a wide range of visible light with large extinction coefficients. (2) Excitation energy on the ZnPor part is transferred to the ZnPc moiety almost quantitatively. (3) CS takes place with a 93% efficiency to the ZnPor dimer from the ZnPc directly excited or after ENT process. (4) The high free energy state of the CS species associated with the long lifetime is ideal for maximum use of the light energy for photovoltaic cell application.

The present results indicate that the strong electronic interaction in the D−A pair and the small reorganization energy in the ET reactions are properties essential to the rapid CS for the

ZnPc−ZnPor dyad system of small energy gap. The equilibrium between the LE and CS state of the comparable energy levels results in the effective elongation of the time constant of the CS state for D−A pair. These findings serve as a new strategy for designing efficient artificial photosynthetic systems. Although the present k_{CS} and k_{CR} rate constants with a large electronic coupling matrix element of $V = 16$ meV could be interpreted by the nonadiabatic electron transfer theory with $\Delta G_{CS} \sim 0$, the exciton−exciton interaction and/or charge resonance interaction between Por and Pc were suggested. The unique structures including slipped-cofacial ZnPor dimer and direct linking of Pc and Por moieties serve as important factors for both efficient charge separation and maximum use of photon energy.

Acknowledgment. We thank Mr. M. Yasuda for measurements of the fluorescence lifetime. We express sincere gratitude to Prof.'s N. Mataga and T. Okada for their discussion on the strong electronic interaction and exciplex. This work was partly supported by Grand-in-Aids for Research in Priority Area (No. 432) (H.M.) and for Scientific Research (A) (No. 15205020) (Y.K.) from the Ministry of Education, Culture, Sports, Science, and Technology (MEXT) of the Japanese Government.

References and Notes

(1) (a) *The Photosynthetic Reaction Center*; Deisenhofer, J., Norris, J. R., Eds.; Academic Press: New York, 1993; Vols. I and II. (b) Tran-Thi, T. *Coord. Chem. Rev.* **1997**, *160*, 553.

(2) (a) Wasielewski, M. R. *Chem. Rev.* **1992**, *92*, 435. (b) Rybtchinski, B.; Sinks, L. E.; Wasielewski, M. R. *J. Am. Chem. Soc.* **2004**, *126*, 12268. (c) Fuller, M. J.; Sinks, L. E.; Rybtchinski, B.; Giaimo, J. M.; Li, X.; Wasielewski, M. R. *J. Phys. Chem. A* **2005**, *109*, 970.

(3) (a) Gust, D.; Moore, T. A.; Moore, A. L. *Acc. Chem. Res.* **2001**, *34*, 40. (b) Kuciauskas, D.; Liddell, P. A.; Lin, S.; Johnson, T. E.; Weghorn, S. J.; Lindsey, J. S.; Moore, A. L.; Moore, T. A.; Gust, D. *J. Am. Chem. Soc.* **1999**, *121*, 8604. (c) Liddell, P. A.; Kodis, G.; Moore, A. L.; Moore, T. A.; Gust, D. *J. Am. Chem. Soc.* **2002**, *124*, 7668.

(4) (a) Osuka, A.; Marumo, S.; Mataga, N.; Taniguchi, S.; Okada, T.; Yamazaki, I.; Nishimura, Y.; Ohno, T.; Nozaki, K. *J. Am. Chem. Soc.* **1996**, *118*, 155. (b) Osuka, A.; Mataga, N.; Okada, T. *Pure. Appl. Chem.* **1997**, *69*, 797. (c) Nakashima, S.; Taniguchi, S.; Okada, T.; Osuka, A.; Mizutani, Y.; Kitagawa, T. *J. Phys. Chem. A* **1999**, *103*, 9184.

(5) (a) Imahori, H.; Sakata, Y. *Eur J. Org. Chem.* **1999**, *2445*, 5. (b) Imahori, H.; Tkachenko, N. V.; Vehmanen, V.; Tamaki, K.; Lemmetyinen, H.; Sakata, Y.; Fukuzumi, S. *J. Phys. Chem. A* **2001**, *105*, 1750. (c) Kesti, T. J.; Tkachenko, N. V.; Vehmanen, V.; Yamada, H.; Imahori, H.; Fukuzumi, S.; Lemmetyinen, H. *J. Am. Chem. Soc.* **2002**, *124*, 8067. (d) Imahori, H. *J. Phys. Chem. B* **2004**, *108*, 6130.

(6) (a) Kobuke, Y.; Miyaji, H. *J. Am. Chem. Soc.* **1994**, *116*, 4111. (b) Kobuke, Y.; Miyaji, H. *Bull Chem. Soc. Jpn.* **1996**, *69*, 3563. (c) Kobuke, Y.; Ogawa, K. *Bull. Chem. Soc. Jpn.* **2003**, *76*, 689. (d) Ogawa, K.; Kobuke, Y. *Angew. Chem. Int. Ed.* **2000**, *39*, 4070.

(7) Ozeki, H.; Nomoto, A.; Ogawa, K.; Kobuke, Y.; Murakami, M.; Hosoda, K.; Ohtani, M.; Nakashima, S.; Miyasaka, H.; Okada T. *Chem.—Eur. J.* **2004**, *10*, 6393.

(8) (a) Gaspard, S. C. R. *Acad. Sci. Paris* **1984**, *298*, 379. (b) Radzki, S.; Gaspard, S.; Giannotti, C. *J. Chem. Res. Synopses* **1986**, *10*, 360. (c) Tran-Thi, T. H.; Lipskier, J. F.; Houde, D.; Pepin, C.; Keszei, E.; Jay-Gerin, J. P. *J. Chem. Soc., Faraday Trans*. **1992**, *88*, 2129.

(9) (a) Gaspard, S.; Giannotti, C.; Maillard, P.; Schaeffer, C.; Tran-Thi, T.-H. *J. Chem. Soc., Chem. Commun.* **1986**, 1239. (b) Tran Thi, T. H.; Desforge, C.; Thiec, C.; Gaspard, S. *J. Phys. Chem.* **1989**, *93*, 1226. (c) Li, L.; Shen, S.; Yu, Q.; Zhou, Q.; Xu, H. *J. Chem. Soc., Chem. Commun.* **1991**, 619. (d) Tian, H.; Zhou, Q.; Shen, S.; Xu, H. *J. Photochem. Photobiol. A: Chem.* **1993**, *72*, 163. (e) Yang, S. I.; Li, J.; Cho, H. S.; Kim, D.; Bocian, D. F.; Holten, D.; Lindsey, J. S. *J. Mater. Chem.* **2000**, *10*, 283. (f) Sutton, J. M.; Boyle, R. W. *Chem. Commun.* **2001**, 2014. (g) Tomé, J. P. C.; Pereira, A. M. V. M.; Alonso, C. M. A.; Neves, M. G. P. M. S.; Tomé, A. C.; Silva, A. M. S.; Cavaleiro, J. A. S.; Martínez-Díaz, M. V.; Torres, T.; Rahman, G. M. A.; Ramey, J.; Guldi D. M. *Eur. J. Org. Chem.*. **2006**, 257.

(10) (a) Tian, H.; Zhou, Q.; Shen, S.; Xu, H. *Chin. J. Chem.* **1996**, *14*, 412. (b) Li, X.; Zhou, Q.; Tian, H.; Xu, H. *Chin. J. Chem.* **1998**, *16*, 97.

(11) (a) Dalton, J.; Milgrom, L. R. *J. Chem. Soc. Chem. Commun.* **1979**, 609. (b) Harrimann, A.; Hosie, R. J. *J. Photochem.* **1981**, *15*, 163. (c) Bergkamp, M. A.; Dalton, J.; Netzel, T. L. *J. Am. Chem. Soc.* **1982**, *104*, 253. (d) Rodriguez, J.; Kirmaier, C.; Johnson, M. R.; Friesner, R. A.; Holten, D.; Sessler, J. L. *J. Am. Chem. Soc.* **1991**, *113*, 1652. (e) Kamioka, K.; Cormier, R. A.; Lutton, T. W.; Connolly, J. S. *J. Am. Chem. Soc.* **1992**, *114*, 4414. (f) D'Souza F.; Deviprasad, G. R.; Hsieh, Y.-Y. *Chem. Commun.* **1997**, 533. (g) Wynne, K.; LeCours, S. M.; Galli, C.; Therien, M. J.; Hochstrasser, R. M. *J. Am. Chem. Soc.* **1995**, *117*, 3749. (h) Macpherson, A. N.; Liddell, P. A.; Lin, S.; Noss, L.; Seely, G. R.; DeGraziano, J. M.; Moore, A. L.; Moore, T. A.; Gust, D. *J. Am. Chem. Soc.* **1995**, *117*, 7202.

(12) (a) Osuka, A.; Nakajima, S.; Maruyama, K.; Mataga, N.; Asahi, T. *Chem. Lett.* **1991**, *1003*. (b) Osuka, A.; Yamada, H.; Maruyama, K.; Mataga, N.; Asahi, T.; Yamazaki, I.; Nishimura, Y. *Chem. Phys. Lett.* **1991**, *181*, 419. (c) Osuka, A.; Nakajima, S.; Maruyama, K.; Mataga, N.; Asahi, T.; Yamazaki, I.; Nishimura, Y.; Ohno, T.; Nozaki, K. *J. Am. Chem. Soc.* **1993**, *115*, 4577. (d) Osuka, A.; Zhang R.-P.; Maruyama, K.; Ohno, T.; Nozaki, K. *Bull. Chem. Soc. Jpn.* **1993**, *66*, 3773. (e) Wiederrecht, G. P.; Niemczyk, M. P.; Svec, W. A.; Wasielewski, M. R. *J. Am. Chem. Soc.* **1996**, *118*, 81.

(13) (a) Mataga, N.; Chosrowjan, H.; Shhibata, Y.; Yoshida, N.; Osuka, A.; Kikuzawa, T.; Okada, T. *J. Am. Chem. Soc.* **2001**, *123*, 12422. (b) Mataga, N.; Chosrowjan, H.; Taniguchi, S.; Shibata, Y.; Yoshida, N.; Osuka, A.; Kikuzawa, T.; Okada, T. *J. Phys. Chem. A* **2002**, *106*, 12191.

(14) Yoshida, N.; Ishizuka, T.; Yofu, K.; Murakami, M.; Miyasaka, H.; Okada, T.; Nagata, Y.; Itaya, A.; Cho, H. S.; Kim, D.; Osuka A. *Chem.—Eur. J.* **2003**, *9*, 2854.

(15) Kameyama, K.; Satake, A.; Kobuke, Y. *Tetrahedron Lett.* **2004**, *45*, 7617.

(16) Satake, A.; Kobuke, Y. *Tetrahedron* **2005**, *61*, 13.

(17) (a) Miyasaka, H.; Moriyama, T.; Kotani, S.; Muneyasu, R.; Itaya, A. *Chem. Phys. Lett.* **1994**, *225*, 315. (b) Miyasaka, H.; Moriyama, T.; Itaya, A. *J. Phys. Chem.* **1996**, *100*, 12609.

(18) (a) Takagi, Y.; Sumitani, M.; Nakashima, N.; O'Connor, D. V.; Yoshihara, K. *Appl. Phys. Lett.* **1983**, *42*, 489. (b) Takagi, Y.; Sumitani, M.; Nakashima, N.; Yoshihara, K. *Rev. Laser. Eng.* **1982**, *10*, 419 (in Japanese).

(19) Miyasaka, H.; Murakami, M.; Okada, T.; Nagata, Y.; Itaya, A.; Kobatake, S.; Irie, M. *Chem. Phys. Lett.* **2003**, *371*, 40.

(20) (a) M., Kasha *Radiat. Res.* **1963**, *20*, 55. (b) Kasha, M.; Rawls, H. R.; Ashraf El-Bayoumi, M. *Pure Appl. Chem.* **1965**, *11*, 371.

(21) (a) Förster, T. *Ann. Phys.* **1948**, *2*, 55. (b) Förster, T. *Z. Naturforsch., A* **1949**, *4*, 321. (c) Förster, T. *Discuss. Faraday Soc.* **1959**, *27*, 7.

(22) *Energy transfer parameters of aromatic compounds*; Berlman, I. B. Ed.; Academic Press: New York, 1973.

(23) (a) Nakano, A.; Osuka, A.; Yamazaki, T.; Nishimuara, Y.; Akimoto, S.; Yamazaki, I.; Itaya, A.; Murakami, M.; Miyasaka, H. *Chem.—Eur. J.* **2001**, *7*, 3134. (b) Nakano, A.; Yasuda, Y.; Yamazaki, T.; Akimoto, S.; Yamazaki, I.; Miyasaka, H.; Itaya, A.; Murakami, M.; Osuka, A. *J. Phys. Chem. A* **2001**, *105*, 4822.

(24) Cho, H. S.; Rhee, H.; Song, J. K.; Min, C.-K.; Takase, M.; Aratani, N.; Cho, S.; Osuka, A.; Joo, T.; Kim, D. *J. Am. Chem. Soc.* **2003**, *125*, 5849.

(25) *Handbook of Photochemistry*, 2nd ed.; Murov, S. L., Carmichael I., Hug, G. L., Eds.; Marcel Dekker: New York, 1993.

(26) Nojiri, T.; Alam, M. M.; Konami, H.; Watanabe, A.; Ito, O. *J. Phys. Chem. A* **1997**, *101*, 7943.

(27) Physical Chemistry. *The Porphyrin*; Dolphin, D., Ed.; Academic Press: New York, 1978; Vol. V, Part C.

(28) Ohno, T.; Kato, S.; Lichtin, N. N. *Bull. Chem. Soc. Jpn.* **1982**, *55*, 2753.

(29) Ohtani, H.; Kobayashi, T.; Ohno, T.; Kato, S.; Tanno, T.; Yamada, A. *J. Phys. Chem.* **1984**, *88*, 4431.

(30) The fluorescence decay curves of ZnPc−ZnPor were accumulated over 3 days, because the quantum efficiency of the photomultiplier with microchannel plates (Hamamatsu R2809) at $\lambda > 700$ nm and the fluorescence quantum yield of the sample are very low, and then the photodegradation species may contribute to this long lifetime component of 4.5 ns.

(31) Birks, J. B. *Photophysics of Aromatic Molecules*; Wiley-Interscience: London, 1970; p 303.

(32) Weller, A. *Z. Phys. Chem. (N. Y.)* **1982**, *133*, 93.

(33) Marcus, R. A.; Sutin, N. *Biochem. Biophys. Acta* **1985**, *811*, 265.

(34) (a) Ulstrup, J.; Jortner, J. *J. Chem. Phys.* **1975**, *63*, 4358. (b) Jortner, J. *J. Chem. Phys.* **1976**, *64*, 4860.

(35) Asahi, T.; Ohkohchi, M.; Matsusaka, R.; Mataga, N.; Zhang, R. P.; Osuka, A.; Maruyama, K. *J. Am. Chem. Soc.* **1993**, *115*, 5665.

(36) Mataga, N. In *The exciplex*; Gordon, M., Ware, W. R., Eds.; Academic Press Inc.: New York, 1974; p 113.

(37) Nagakura, S. In *Excited States*; Lim, E. D., Ed.; Academic Press Inc.: New York, 1975; Vol. 2, p 321.

(38) Mataga, N.; Okada, T.; Yamamoto, N. *Chem. Phys. Lett.* **1967**, *1*, 119.